Enhanced Open Circuit Voltage and Efficiency of Donor–Acceptor Copolymer Solar Cells by Using Indene–C60 Bisadduct

ARTICLE *in* CHEMISTRY OF MATERIALS · MAY 2012

Impact Factor: 8.35 · DOI: 10.1021/cm300355e

6 AUTHORS, INCLUDING:

Hao Xin
University of Washington Seattle
22 PUBLICATIONS **1,138** CITATIONS
SEE PROFILE

Selvam Subramaniyan
University of Washington Seattle
33 PUBLICATIONS **867** CITATIONS
SEE PROFILE

Safa Shoaee
Imperial College London
27 PUBLICATIONS **670** CITATIONS
SEE PROFILE

CHEMISTRY OF MATERIALS

Article

pubs.acs.org/cm

Enhanced Open Circuit Voltage and Efficiency of Donor–Acceptor Copolymer Solar Cells by Using Indene-C60 Bisadduct

Hao Xin,[†] Selvam Subramaniyan,[†] Tae-Woo Kwon,[†,§] Safa Shoaee,[‡] James R. Durrant,[‡] and Samson A. Jenekhe[†,*]

[†]Department of Chemical Engineering and Department of Chemistry, University of Washington, Seattle, Washington 98195-1750, United States

[‡]Center for Plastic Electronics, Department of Chemistry, Imperial College London, London SW7 2AZ, United Kingdom

ABSTRACT: The photovoltaic properties of bulk heterojunction solar cells using indene-C60 bisadduct (ICBA) as the electron acceptor were investigated by using three donor–acceptor copolymers (PSEHTT, PSOTT, and PSOxTT) in comparison with $PC_{61}BM$-based solar cells. The open circuit voltage of the copolymer:ICBA devices was 0.82–0.92 V, which is 0.25 V enhanced compared to the copolymer:PCBM solar cells. Compared to PCBM-based solar cells, the photocurrent density of ICBA-based devices was significantly increased in the case of PSEHTT but decreased in PSOTT and PSOxTT. This variation of photocurrent density with the copolymer structure was correlated with the charge photogeneration efficiency as determined by transient absorption spectroscopy. A power conversion efficiency of 5.4% was achieved in PSEHTT:ICBA solar cells, which represents a 50% enhancement in efficiency compared to $PC_{61}BM$ devices. Our results demonstrate that ICBA can significantly increase the open circuit voltage, current density, and power conversion efficiency of donor–acceptor copolymer-based BHJ solar cells.

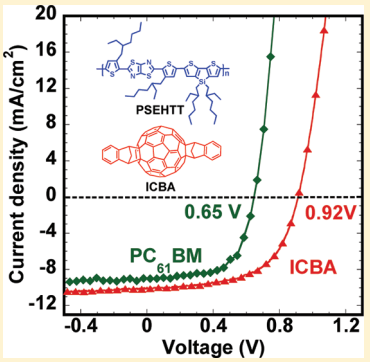

KEYWORDS: *charge photogeneration, fullerene bisadduct, open circuit voltage, polymer solar cell, thiazolothiazole polymers, transient absorption spectroscopy*

INTRODUCTION

Conjugated polymer-based photovoltaic cells are of growing interest as potential low cost solar energy to electricity conversion technologies.[1−5] State-of-the-art polymer solar cells, the so-called bulk heterojunction (BHJ) devices, typically consist of blends of an electron-donating and hole-transporting π-conjugated polymer (*p-type* semiconductor) and an electron-accepting and electron-transporting fullerene derivative (*n-type* semiconductor) as the active layer.[1−4] Several factors are essential to achieve a high power conversion efficiency in such a BHJ solar cell,[1] including (i) efficient light harvesting which can increase the photocurrent density; (ii) sufficient energy offset between the LUMO level of the fullerene derivative and the HOMO level of the polymer semiconductor to facilitate a high open circuit voltage; (iii) existence of a bicontinuous nanoscale phase-separated morphology of the BHJ polymer blend to enable efficient charge separation and high photocurrent; and (iv) high bipolar carrier mobilities within the phase-separated BHJ polymer blend to maximize charge collection and attain a high fill factor.[1] Improvement of light absorption has been largely addressed by the synthesis of narrow band gap conjugated polymers with donor–acceptor architecture[2,6−15] while optimal nanomorphology is achieved by various film processing approaches, such as thermal annealing,[16] self-assembled nanowires,[17−20] and the use of a processing additive.[10,21−24] BHJ polymer solar cells with a power conversion efficiency in the range of 6–8% have been achieved by a combination of these strategies.[8,9,25,26]

Compared to the improvements in the photocurrent density and fill factor of BHJ polymer solar cells, advances in improvement of the open circuit voltage have been relatively slow. This is because the most efficient BHJ solar cells have used one of the fullerene derivatives [6,6]-phenyl-C_{61}-butyric acid methyl ester ($PC_{61}BM$) and [6,6]-phenyl-C_{71}-butyric acid methyl ester ($PC_{71}BM$) (Figure 1a) as the electron-accepting and electron-transporting component. Due to the fixed LUMO energy levels of PCBM (3.9 eV, Figure 1b)[27] and the requirement of a certain amount of LUMO energy offset for efficient exciton dissociation,[1] the room for tuning the energy level difference between the LUMO of PCBM and the HOMO of the polymer to increase the open circuit voltage has been limited. Recently a new fullerene derivative, indene-C_{60} bisadduct (ICBA),[27,28] which has a LUMO energy level of 3.7 eV[27] below vacuum, has been reported. By using ICBA as an electron-acceptor, the open circuit voltage of P3HT-based BHJ solar cells was increased from 0.58 to 0.84 V and the efficiency was thus improved from 3.8% to 6.5% PCE,[8] demonstrating the great potential of this new fullerene derivative. However, ICBA-based BHJ devices are yet to be explored with donor–acceptor copolymer semiconductors having a smaller band gap than P3HT and good match of HOMO/LUMO energy levels.

Received: July 6, 2011
Revised: May 6, 2012
Published: May 17, 2012

dx.doi.org/10.1021/cm300355e | *Chem. Mater.* 2012, 24, 1995–2001

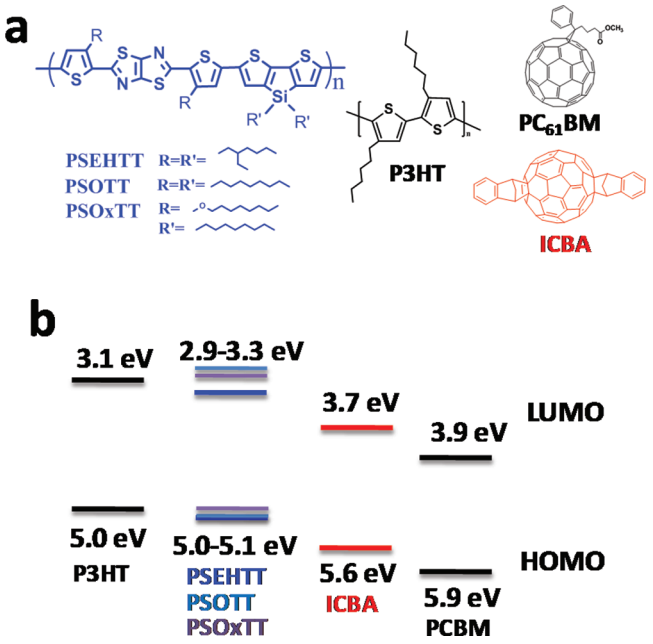

Figure 1. (a) Molecular structures and (b) HOMO/LUMO energy levels (below vacuum) of PSEHTT, PSOTT, PSOxTT, P3HT, and fullerene derivatives (ICBA, $PC_{61}BM$, and $PC_{71}BM$). The HOMO/LUMO energy levels of P3HT and PSEHTT were estimated from the onset oxidation potentials in cyclic voltammetry and their optical band gaps; the energy levels of ICBA and PCBM are from ref 33.

We recently reported the synthesis, charge transport, and photovoltaic properties of a series of thiazolothiazole–dithienosilole donor–acceptor copolymers, poly[(4,4′-bis(3-(2-ethyl-hexyl)dithieno[3,2-*b*:″,3′-*d*]silole)-2,6-diyl-*alt*-(2,5-bis-(3-(2-ethyl-hexyl)thiophen-2-yl)thiazolo[5,4-*d*]thiazole)] (**PSEHTT**), poly[(4,4′-bis(2-octyl)dithieno[3,2-*b*:″,3′-*d*]silole)-2,6-diyl-*alt*-(2,5-bis(3-octylthiophen-2-yl)thiazolo[5,4-*d*]-thiazole)] (**PSOTT**), and poly[(4,4′-bis(2-octyl)dithieno[3,2-*b*:″,3′-*d*]silole)-2,6-diyl-*alt*-(2,5-bis(3-octyloxythiophen-2-yl)-thiazolo[5,4-*d*]thiazole)] (**PSOxTT**) (Figure 1a).[29] These D–A copolymers have a band gap of 1.7–1.8 eV and a field-effect hole mobility of 0.03–0.12 $cm^2/(V{\cdot}s)$. Efficient solar cells with a power conversion efficiency of 5.0% were observed in PSEHTT:$PC_{71}BM$ blends.[29] The HOMO/LUMO energy levels of PSEHTT, PSOTT, and PSOxTT are 5.1/3.3, 5.1/2.9, and 5.0/3.0 eV, respectively, suggesting the potential for a good match with ICBA. In this paper, we report studies of BHJ solar cells comprising these D–A copolymers and ICBA. We show that by replacing $PC_{61}BM$ with ICBA, the open circuit voltage of all the solar cells is increased by 0.23–0.27 V to up to 0.92 V. However, the overall photovoltaic efficiency varied from polymer to polymer. PSEHTT:ICBA solar cells achieved a 5.4% power conversion efficiency, which represents a 50% enhancement compared to the corresponding $PC_{61}BM$ devices. The efficiency observed in PSOTT:ICBA and PSOxTT:ICBA solar cells was much lower than those of the corresponding $PC_{61}BM$ devices, mainly due to the greatly reduced short-circuit current density. The film morphology and transient absorption spectroscopy of the BHJ polymer blends were explored to understand the observed difference in the photovoltaic performance. These results demonstrate that the open circuit voltage, current density, and thus efficiency of bulk heterojunction polymer solar cells can be significantly increased by combining ICBA with a donor polymer other than poly(3-hexylthiophene). It is interesting to note that while our manuscript was under review, a few papers by other research groups[30−32] have appeared and similarly explored the use of ICBA toward improvement of power conversion efficiency of donor–acceptor copolymer solar cells.

EXPERIMENTAL SECTION

The synthesis and characterization of PSEHTT, PSOTT, and PSOxTT were previously reported.[29] The number average molecular weight (M_n) and polydispersity (PDI) of PSEHTT, PSOTT, and PSOxTT were 33.9 kDa and 3.9, 10.8 kDa and 3.3, and 24.3 kDa and 2.0, respectively. The fullerene derivatives, ICBA (99.0%), $PC_{61}BM$ (99.5%), and $PC_{71}BM$ (99.5%), were purchased from Luminescence Technology Corp. (Taiwan), American Dye Sources (Quebec), and Nano-C (Westwood, MA), respectively. P3HT (M_n = 20–50 kDa) was bought from Rieke Metals (Lincoln, NE). All the materials were used as purchased without further purification. Solar cell devices were fabricated by first spin-coating a 30 nm PEDOT:PSS (Clevios P VP Al 4083, H. C. Stark) buffer layer on top of ITO-coated glass substrates (10 Ω/□, Shanghai B. Tree Tech. Consult Co., Ltd., Shanghai, China) and annealed at 150 °C for 10 min under vacuum. The PSEHTT:fullerene active layer was spin-coated from a solvent mixture of 1,2-dichlorobenzene (ODCB) and 1,8-octanedithiol (ODT) (ODCB:ODT = 100:2.5, v/v) and dried in vacuum for 1 h.[29] The ratio of polymer:fullerene was fixed at 1:2, and the film thickness was about 60 nm, the optimized condition for these polymer solar cells.[29] P3HT:ICBA (1:1) solar cells with a thickness of about 190 nm, the same thickness as reported in the best P3HT/ICBA solar cell,[8] were fabricated for comparison. The devices were finished by the deposition of the cathode, consisting of 1.0 nm LiF and 100 nm aluminum layer, in a thermal evaporator in a vacuum of 8×10^{-7} Torr. Each substrate contained four pixels with an active area of 9 mm^2. Current–voltage characteristics were measured by using a HP4155A semiconductor parameter analyzer (Yokogawa Hewlett-Packard, Tokyo). The light intensity of 1.5 A.M. sunlight from a filtered Xe lamp was calibrated by a Si photodiode calibrated at the National Renewable Energy Laboratory (NREL). The external quantum efficiency (EQE) was measured on an EQX-10 (PV Measurement, Inc.) EQE/IPCE spectral response system. All the characterization steps were carried out under ambient laboratory air. UV–vis absorption spectra were recorded on a Perkin-Elmer model Lambda 900 UV/vis/near-IR spectrophotometer. Bright-field transmission electron images (BF-TEM) were measured on An FEI Tecnai G^2 F20 TEM at 200 kV accelerating voltage. The images were slightly defocused to enhance the phase contrast and were then acquired with a CCD camera and recorded with Gatan DigitalMicrograph software with proper exposure time.

Transient absorption decays were measured by exciting the sample film, under a nitrogen atmosphere, with a commercially available optical parametric oscillator (Oppolette) pumped by a Nd:Yag laser. The time duration of the pump-pulses was 20 ns. The excitation wavelength used was 550 nm, with a pump intensity of 0.4–75 $\mu J{\cdot}cm^{-2}$ and a repetition frequency of 20 Hz. A 100 W quartz halogen lamp (Bentham, IL 1) with a stabilized power supply (Bentham, 605) was used as a probe light source, with a pump wavelength of 730 nm used. The probe light passing through the sample film was detected with a silicon photodiode (Hamamatsu Photonics, S1722-01). The signal from the photodiode was preamplified and sent to the main amplification system with an electronic band-pass filter (Costronics Electronics). The amplified signal was collected with a digital oscilloscope (Tektronics, TDS220), which was synchronized with a trigger signal of the pump laser pulse from a photodiode (Thorlabs Inc., DET210). To reduce stray light, scattered light, and sample emission, two monochromators and appropriate optical cutoff filters were placed before and after the sample.

RESULTS AND DISCUSSION

PSEHTT-Based Solar Cells. Representative current density–voltage (J–V) curves and absorption spectra of

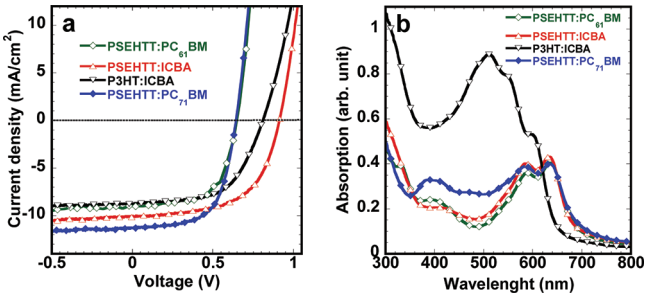

Figure 2. (a) $J-V$ curves of PSEHTT and P3HT solar cells using different fullerene derivatives as indicated in the figure. (b) Absorption spectra of polymer:fullerene blend films measured directly from the devices in (a) in transmission mode by using ITO/PEDOT substrate as a reference.

Table 1. Comparison of Performance of PSEHTT, PSOTT, and PSOxTT Solar Cells Using Various Fullerene Derivatives

active layer	J_{sc} (mA/cm^2)	V_{oc} (V)	FF	PCE (%)[a]
PSEHTT:$PC_{61}BM$ (1:2)	8.94	0.65	0.62	3.61 ± 0.09
PSEHTT:ICBA (1:2)	10.1	0.92	0.58	5.36 ± 0.06
P3HT:ICBA (1:1)	8.95	0.81	0.56	4.11 ± 0.04
PSEHTT:$PC_{71}BM$ (1:2)	11.2	0.64	0.62	4.47 ± 0.09
PSOTT:$PC_{71}BM$ (1:2)	11.3	0.57	0.52	3.29 ± 0.09
PSOTT:ICBA (1:2)	6.60	0.84	0.46	2.52 ± 0.07
PSOxTT:$PC_{71}BM$ (1:2)	6.67	0.59	0.52	2.08 ± 0.07
PSOxTT:ICBA (1:2)	4.64	0.82	0.44	1.68 ± 0.08

[a]Average and standard deviation based on four devices.

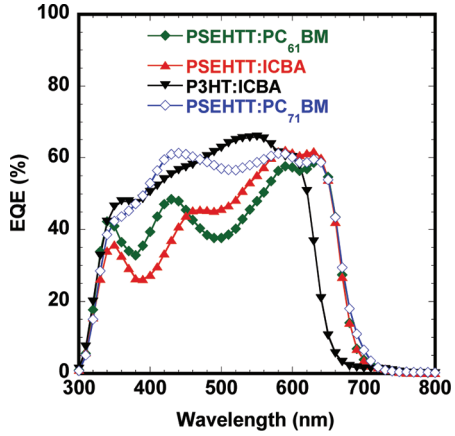

Figure 3. EQE spectra of PSEHTT:fullerene (ICBA, $PC_{61}BM$, $PC_{71}BM$) and P3HT:ICBA solar cells.

PSEHTT:$PC_{61}BM$, PSEHTT:ICBA, P3HT:ICBA, and PSEHTT:$PC_{71}BM$ solar cells are shown in Figure 2a. The photovoltaic parameters for all the BHJ devices are summarized in Table 1. The copolymer:fullerene blend composition was fixed at 1:2 (w/w) because our previous studies of these copolymer:fullerene BHJ devices showed it to be optimum.[29] We also note that P3HT solar cells reported here had a thickness of about 190 nm, similar to that reported in the literature,[8] and P3HT solar cells with comparable thickness to that of PSEHTT solar cells gave similar performance to that of the 190 nm devices. The average power conversion efficiencies (PCE) observed in PSEHTT:$PC_{61}BM$ (1:2), PSEHTT:ICBA (1:2), P3HT:ICBA (1:1), and PSEHTT:$PC_{71}BM$ (1:2) solar

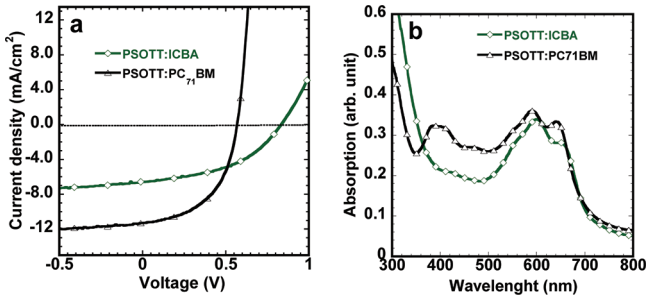

Figure 4. (a) $J-V$ curves of PSOTT:ICBA (1:2) and PSOTT:$PC_{71}BM$ (1:2) solar cells. (b) Absorption spectra of PSOTT:ICBA (1:2) and PSOTT:$PC_{71}BM$ (1:2) blend films measured directly from the devices in (a) using the ITO/PEDOT substrate as a reference.

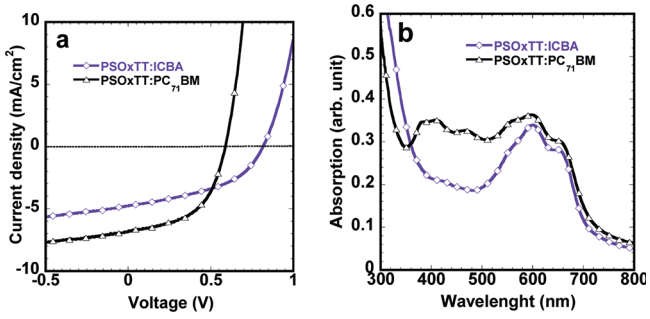

Figure 5. (a) $J-V$ curves of PSOxTT:ICBA (1:2) and PSOxTT:$PC_{71}BM$ (1:2) solar cells. (b) Absorption spectra of PSOxTT:ICBA (1:2) and PSOxTT:$PC_{71}BM$ (1:2) blend films measured directly from the devices in (a) using ITO/PEDOT substrate as a reference.

cells are 3.6%, 5.4%, 4.1%, and 4.5%, respectively. The external quantum efficiency (EQE) spectra of the four different BHJ devices are shown in Figure 3. All the devices showed high photoconversion efficiency with peak EQE values of over 60%. The EQE spectra followed the absorption spectra (Figure 2b) very well. The J_{sc} value calculated by integrating the EQE curves with an AM1.5G reference spectrum gave ~5% error compared to the corresponding J_{sc} value obtained from the $J-V$ measurements, and this can be explained by the spectral mismatch of the solar simulator.[29]

It is interesting that replacing $PC_{61}BM$ with ICBA in PSEHTT-based solar cells results in a 42% increase in the open circuit voltage, from 0.65 to 0.92 V. The large enhancement of the V_{oc} in PSEHTT:ICBA devices is in good agreement with the 0.2 eV LUMO energy level difference between PCBM and ICBA and the smaller loss in PSEHTT exciton energy (Figure 1). The current density in PSEHTT:ICBA solar cells is also increased from 8.94 to 10.1 mA/cm^2, due largely to the slightly higher absorption intensity in this film (Figure 2b) and slightly smaller loss in PSEHTT exciton energy. Although replacing $PC_{61}BM$ with ICBA resulted in a decrease of FF from 0.62 to 0.58, the 42% enhancement in V_{oc} and the 11% enhancement in J_{sc} together increased the power conversion efficiency by 50% from 3.61% to 5.36%.

Compared to P3HT:ICBA solar cells, the current density and open circuit voltage of PSEHTT:ICBA solar cells increased by 13% (from 8.95 to 10.1 mA/cm^2) and 14% (from 0.81 to 0.92 V), respectively, leading to a 30% enhancement in power conversion efficiency. It is obvious that the higher current density and open circuit voltage in PSEHTT:ICBA solar cells come from the more red-shifted absorption (Figure 2b), lower

dx.doi.org/10.1021/cm300355e | Chem. Mater. 2012, 24, 1995−2001

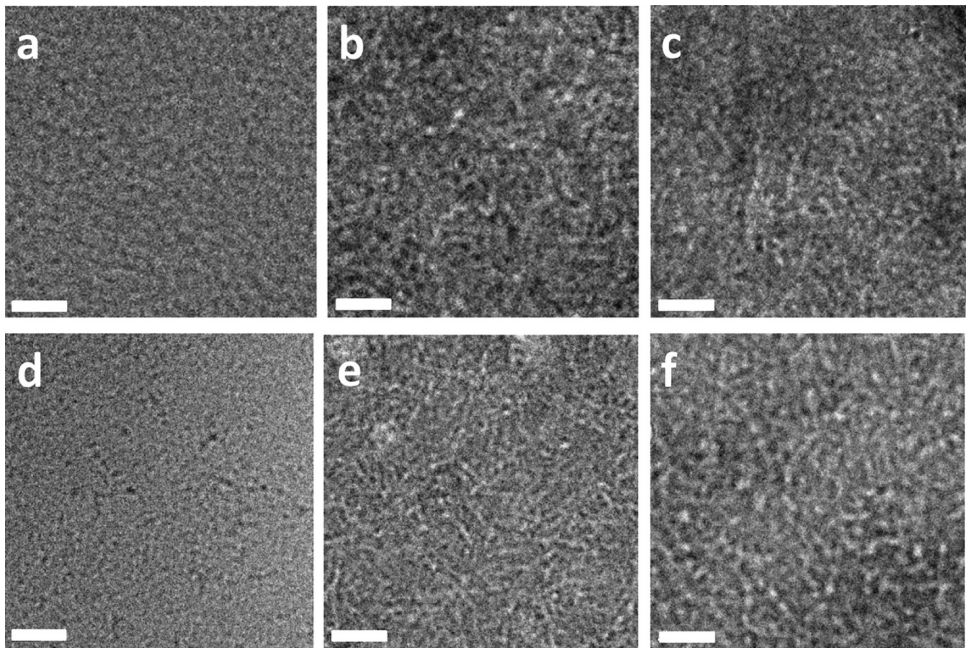

Figure 6. Bright field TEM images of blend films of (a) PSEHTT:ICBA, (b) PSOTT:ICBA, (c) PSOxTT:ICBA, (d) PSEHTT:$PC_{71}BM$, (e) PSOTT:$PC_{71}BM$, and (f) PSOxTT:$PC_{71}BM$ (f). The scale bars are 100 nm for all the images.

lying HOMO energy level of PSEHTT, and smaller exciton energy (Figure 1). The exciton energy of PSEHTT is 0.2 eV lower compared to P3HT, which means that less of the energy harvested is lost by conversion. We note that the peak efficiency observed in P3HT:ICBA solar cells was 6.5%,[8] which is much higher than our 4.1% (Table 1); this suggests that better performance can be expected from the PSEHTT:ICBA system by further device optimization and device testing in an inert environment.

The use of fullerene derivative $PC_{71}BM$ instead of $PC_{61}BM$ as the electron accepting material, due to the absorption of $PC_{71}BM$ in the range of 350−550 nm (Figure 2b), resulted in increased current density from 10.4 to 11.2 mA/cm^2 (Table 1) in PSEHTT:$PC_{71}BM$ solar cells while the V_{oc} and FF were not changed. The $PC_{71}BM$ devices were 13% more efficient. We note that due to the larger device area (9 mm^2) in the present study and batch to batch difference, the PCE (4.5%) of PSEHTT:$PC_{71}BM$ measured in this report is slightly lower than in our previous report (5.0%).[29] We also note that indene-C_{70} bisadduct with a similar absorption spectrum as $PC_{71}BM$ and comparable energy levels as ICBA has been recently reported.[33] Thus, even higher efficiency can be expected in PSEHTT:indene-C_{70} solar cells since the indene-C_{70} bisadduct as the electron-accepting material could increase the current density and open circuit voltage at the same time.

PSOTT:ICBA Solar Cells. Figure 4 shows the current density−voltage (J−V) curves and absorption spectra of PSOTT:ICBA (1:2) and PSOTT:$PC_{71}BM$(1:2) solar cells. The photovoltaic parameters of these devices are also summarized in Table 1. The J_{sc}, V_{oc}, and FF observed in PSOTT:ICBA solar cells were 6.60 mA/cm^2, 0.84 V, and 0.46, respectively, resulting in a PCE of 2.52%. The J_{sc}, V_{oc}, FF, and PCE obtained in the control PSOTT:$PC_{71}BM$ device were 11.3 mA/cm^2, 0.57 V, 0.52, and 3.29%, respectively. Similar to PSEHTT solar cells, the replacement of $PC_{71}BM$ by $IC_{61}BA$ results in increase of the open circuit voltage of PSOTT solar cells by 0.27 V, from 0.57 to 0.84 V (Table 1 and Figure 4a). This is consistent with the LUMO energy level difference between $PC_{71}BM$ and ICBA (Figure 1). However, the current density of PSOTT:ICBA solar cells significantly decreased by 42% (from 11.3 to 6.60 mA/cm^2), which is the main factor for the overall 25% decrease in the power conversion efficiency. We know that the relatively low absorption intensity of ICBA compared to $PC_{71}BM$ (Figure 4b) partially accounts for the smaller photocurrent; however, this difference in absorption intensity cannot explain the 42% difference in photocurrent density. We explore another possible explanation later.

PSOxTT:ICBA Solar Cells. The current density−voltage (J−V) curves of PSOxTT:ICBA (1:2) and PSOxTT:$PC_{71}BM$ (1:2) solar cells are shown in Figure 5, and the photovoltaic parameters of these devices are also summarized in Table 1. The J_{sc}, V_{oc}, FF, and PCE measured in PSOxTT:ICBA and PSOxTT:$PC_{71}BM$ solar cells were 4.64 mA/cm^2, 0.82 V, 0.44, and 1.68% and 6.67 mA/cm^2, 0.59 V, 0.52, and 2.08%, respectively. Similar to PSEHTT- and PSOTT-based solar cells, using ICBA instead of $PC_{71}BM$ as the electron acceptor component increased the V_{oc} by 0.23 V, which is in good agreement with the LUMO energy level different between ICBA and $PC_{71}BM$. Unlike PSEHTT but similar to PSOTT solar cells, the power conversion efficiency in PSOxTT:ICBA solar cells is lower, and this mainly comes from the lower current density and lower fill factor (Table 1 and Figure 5). Here too additional factors are also likely at play.

Morphology. To understand the difference in the photovoltaic performance, especially the change in the photocurrent when PCBM is replaced with ICBA, transmission electron microscopy (TEM) was performed to investigate the morphology of the polymer:fullerene blend films. The TEM images are shown in Figure 6. Uniform films with nanofiber-like polymer domains (lighter areas) embedded in amorphous fullerene (darker area) are seen in all the films.

No obvious change in morphology was observed in each pair of the polymer:fullerene blend films, that is, PSEHTT:$PC_{71}BM$ (Figure 6a) versus PSEHTT:ICBA (Figure 6d),

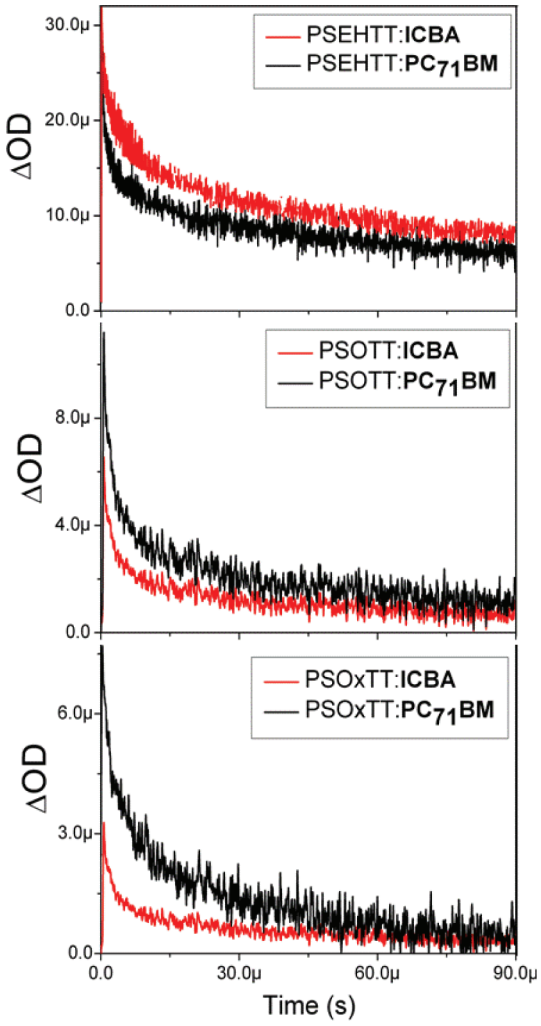

Figure 7. Transient absorption signals of polymer:$PC_{71}BM$ and polymer:ICBA. Decays taken under N_2 atmosphere at $\lambda_{excitation}$ of 550 nm and λ_{probed} of 730 nm with excitation energy of 0.8 μJ cm^{-2}.

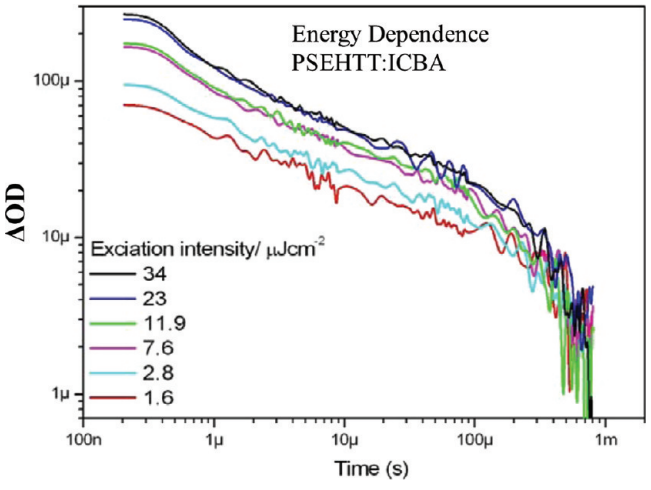

Figure 8. Charge generation of PSEHTT:ICBA blend film as a function of excitation pulse intensity. Films were excited at 550 nm and probed at 730 nm.

PSOTT:$PC_{71}BM$ (Figure 6b) versus PSOTT:ICBA (Figure 6e), and PSOxTT:$PC_{71}BM$ (Figure 6c) versus PSOxTT:ICBA (Figure 6f), indicating that the observed variation in efficiency does not come from the morphology. It is worth noting that the morphology of PSEHTT:fullerene films (Figure 6a,d) is different from the other two polymer:fullerene films. The length of the polymer fiber-like domains in PSEHTT:fullerene films is shorter (20−30 nm) and isolated from each other, whereas the fibers in PSOTT (Figure 6b,e) and PSOxTT (Figure 6, c and d) films are much longer (30−100 nm) and interconnected to each other. We believe that the difference in the morphology of the polymer domains comes from the different orientation of the polymer π-stacking. Our previous X-ray diffraction data revealed that PSEHTT mainly adopts a face-on π-stacking whereas PSOTT and PSOxTT had edge-on π-stacking.[29]

Transient Absorption Spectroscopy. We employed transient optical spectroscopy to consider whether the variation in power conversion efficiency is primarily associated with the charge separation efficiency at the polymer/fullerene interface or the charge collection efficiency by the electrodes. We have previously showed that microsecond transient absorption spectroscopy can be employed to assay the yield of dissociated charges in polymer/fullerene BHJ blend films, and thereby the charge separation efficiency.[34,35] The transient spectra of all three polymer blend films are shown in Figure 7. All films exhibited an absorption maxima around 730 nm which can be assigned to the polymer cations.[29] The amplitude of the transient absorption signal (measured at the polymer's cation absorption maximum) of PSOTT/ICBA and PSOxTT/ICBA films are approximately twofold smaller relative to their PCBM counterparts. In contrast, the signal of PSEHTT:ICBA is approximately 50% higher than that of PSEHTT:PCBM. We note that for all three polymers, the amplitudes of the observed decay transients varied approximately linearly with excitation density (Figure 8), indicating that saturation effects do not distort this comparison. Furthermore, the signals were taken at an excitation wavelength (550 nm) where the film ground state absorbance was either the same or was normalized. Therefore, the increase in signal amplitude cannot be attributed to enhanced light absorption.

Altering the electron acceptor from ICBA to $PC_{71}BM$ had no effect on the peak absorption wavelength (730 nm), consistent with their assignment as polarons of the polymers rather than C_{60}. This is in agreement with previous studies showing that the C_{60} anion absorbs at 1070 nm and exhibits a small extinction coefficient,[36,37] whereas the C_{70} anion absorbs at 1370 nm.[38]

The decay dynamics of all blend films were all oxygen independent and obeyed power law characteristics, consistent with their assignment to polaron rather than triplet absorption, a typical characteristic of nongeminate recombination of dissociated polarons in the presence of an exponential distribution of localized states.[39]

The change in charge generation is in agreement with the trend in J_{sc} values, suggesting that the increase in J_{sc} most probably results from charge separation efficiency rather than collection efficiency. We note that this conclusion is in agreement with our previously reported study.[29,40] In addition, we note that these polymers all exhibit strong photoluminescence quenching when blended with either PCBM or ICBA, indicating efficient exciton dissociation. This therefore suggests that the increase in charge photogeneration and photocurrent generation for this polymer series primarily comes from the difference in geminate recombination at the polymer/fullerene interface, most probably associated with the formation of interfacial charge transfer states,[41,42] following the

dx.doi.org/10.1021/cm300355e | Chem. Mater. 2012, 24, 1995−2001

model we have discussed in more detail elsewhere. We note that the variation between ICBA and PCBM cannot be assigned to the change in interfacial energetics, as we have observed for other systems;[40,41] rather, it appears more likely that this transition results from subtle changes and variation in microstructure and crystallinity between the blend films, as is discussed elsewhere.[43]

From all of the above results we see that the HOMO/LUMO energy differences between ICBA and PCBM can explain the observed substantial enhancement of the photovoltage of the ICBA-based donor−acceptor copolymer solar cells. However, such energy level offsets are not sufficient to account for the increase in photocurrent and power conversion efficiency in the case of PSEHTT and decrease in these parameters in the cases of PSOTT and PSOxTT. We have also examined other factors such as morphology and charge photogeneration and recombination kinetics. However, it remains as yet unclear what the key factor is that controls the photovoltaic performance of polymer/ICBA solar cells. Why one polymer (PSEHTT) works with ICBA to achieve enhanced performance whereas others with similar structure and energy levels (e.g., PSOTT and PSOxTT) do not work remains to be fully understood.

■ CONCLUSIONS

In summary, we have investigated the use of indene-C_{60} bisadduct (ICBA) as the electron acceptor material in BHJ solar cells incorporating thiazolothiazole-based donor−acceptor copolymers. The observed open circuit voltages of all the ICBA-based solar cells at 0.82−0.92 V are increased by about 0.25 V compared to the use of PCBM as electron-acceptor material; the higher lying LUMO energy level of ICBA compared to that of PCBM accounts for this enhancement. The photocurrent density of ICBA-based solar cells was found to greatly depend on the polymer structure, with an increase in PSEHTT solar cells but a decrease in PSOTT and PSOxTT solar cells, resulting in different overall photovoltaic efficiency. The best performance was achieved in PSEHTT:ICBA devices which showed a power conversion efficiency of 5.4%, a 50% enhancement compared to $PC_{61}BM$ devices. The difference in the photocurrent density among these copolymers was found to correlate with the charge photogeneration and primarily to the difference in geminate recombination. The transient optical studies thus indicate that the differences in photovoltaic device performance arise primarily from differences in geminate recombination losses. Our results demonstrate that ICBA can significantly increase the open circuit voltage, current density, and photovoltaic efficiency of donor−acceptor copolymer based BHJ solar cells.

■ AUTHOR INFORMATION

Corresponding Author

*E-mail: jenekhe@u.washington.edu.

Present Address

[§]Department of Chemistry and Center for Organic Devices & Advanced Materials, Kyungsung University, Busan 608-736, Korea

Notes

The authors declare no competing financial interest.

■ ACKNOWLEDGMENTS

This report is based on work (Excitonic Solar Cells) supported by the U.S. Department of Energy, Office of Basic Energy Sciences, Division of Materials Sciences under Award No. DE-FG02-07ER46467. The synthesis and characterization of the donor−acceptor copolymers was supported by the NSF (DMR-0805259) and Solvay S. A.

■ REFERENCES

(1) Gunes, S.; Neugebauer, H.; Sariciftci, N. S. *Chem. Rev.* **2007**, *107*, 1324.
(2) Boudreault, P. L. T.; Najari, A.; Leclerc, M. *Chem. Mater.* **2011**, *23*, 456.
(3) Thompson, B. C.; Frechet, J. M. J. *Angew. Chem., Int. Ed.* **2008**, *47*, 58.
(4) Dennler, G.; Scharber, M. C.; Brabec, C. J. *Adv. Mater.* **2009**, *21*, 1323.
(5) Beljonne, D.; Cornil, J.; Muccioli, L.; Zannoni, C.; Bredas, J. L.; Castet, F. *Chem. Mater.* **2011**, *23*, 591.
(6) Beaujuge, P. M.; Subbiah, J.; Choudhury, K. R.; Ellinger, S.; McCarley, T. D.; So, F.; Reynolds, J. R. *Chem. Mater.* **2010**, *22*, 2093.
(7) Park, S. H.; Roy, A.; Beaupre, S.; Cho, S.; Coates, N.; Moon, J. S.; Moses, D.; Leclerc, M.; Lee, K.; Heeger, A. J. *Nat. Photonics* **2009**, *3*, 297.
(8) Zhao, G. J.; He, Y. J.; Li, Y. F. *Adv. Mater.* **2010**, *22*, 4355.
(9) Zhou, H. X.; Yang, L. Q.; Stuart, A. C.; Price, S. C.; Liu, S. B.; You, W. *Angew. Chem., Int. Ed.* **2011**, *50*, 2995.
(10) Liang, Y. Y.; Feng, D. Q.; Wu, Y.; Tsai, S. T.; Li, G.; Ray, C.; Yu, L. P. *J. Am. Chem. Soc.* **2009**, *131*, 7792.
(11) Wu, P. T.; Bull, T.; Kim, F. S.; Luscombe, C. K.; Jenekhe, S. A. *Macromolecules* **2009**, *42*, 671.
(12) Ahmed, E.; Kim, F. S.; Xin, H.; Jenekhe, S. A. *Macromolecules* **2009**, *42*, 8615.
(13) Subramaniyan, S.; Xin, H.; Kim, F. S.; Jenekhe, S. A. *Macromolecules* **2011**, *44*, 6245.
(14) Ahmed, E.; Subramaniyan, S.; Kim, F. S.; Xin, H.; Jenekhe, S. A. *Macromolecules* **2011**, *44*, 7207.
(15) Xin, H.; Guo, X. G.; Kim, F. S.; Ren, G. Q.; Watson, M. D.; Jenekhe, S. A. *J. Mater. Chem.* **2009**, *19*, 5303.
(16) Li, G.; Shrotriya, V.; Huang, J. S.; Yao, Y.; Moriarty, T.; Emery, K.; Yang, Y. *Nat. Mater.* **2005**, *4*, 864.
(17) Xin, H.; Kim, F. S.; Jenekhe, S. A. *J. Am. Chem. Soc.* **2008**, *130*, 5424.
(18) Xin, H.; Ren, G. Q.; Kim, F. S.; Jenekhe, S. A. *Chem. Mater.* **2008**, *20*, 6199.
(19) Xin, H.; Reid, O. G.; Ren, G. Q.; Kim, F. S.; Ginger, D. S.; Jenekhe, S. A. *ACS Nano* **2010**, *4*, 1861.
(20) Ren, G.; Wu, P.-T.; Jenekhe, S. A. *Chem. Mater.* **2010**, *22*, 2020.
(21) Peet, J.; Kim, J. Y.; Coates, N. E.; Ma, W. L.; Moses, D.; Heeger, A. J.; Bazan, G. C. *Nat. Mater.* **2007**, *6*, 497.
(22) Lee, J. K.; Ma, W. L.; Brabec, C. J.; Yuen, J.; Moon, J. S.; Kim, J. Y.; Lee, K.; Bazan, G. C.; Heeger, A. J. *J. Am. Chem. Soc.* **2008**, *130*, 3619.
(23) Bijleveld, J. C.; Zoombelt, A. P.; Mathijssen, S. G. J.; Wienk, M. M.; Turbiez, M.; de Leeuw, D. M.; Janssen, R. A. J. *J. Am. Chem. Soc.* **2009**, *131*, 16616.
(24) Ren, G. Q.; Ahmed, E.; Jenekhe, S. A. *Adv. Energy Mater.* **2011**, *1*, 946.
(25) Piliego, C.; Holcombe, T. W.; Douglas, J. D.; Woo, C. H.; Beaujuge, P. M.; Frechet, J. M. J. *J. Am. Chem. Soc.* **2010**, *132*, 7595.
(26) Liang, Y.; Xu, Z.; Xia, J.; Tsai, S.-T.; Wu, Y.; Li, G.; Ray, C.; Yu, L. *Adv. Mater.* **2010**, *22*, 1.
(27) He, Y. J.; Chen, H. Y.; Hou, J. H.; Li, Y. F. *J. Am. Chem. Soc.* **2010**, *132*, 1377.
(28) Laird, D. W.; Stegamat, R.; Richter, H.; Vejins, V.; Scott, L.; Lada, T. A. Patent WO 2008/018931 A2, 2008.
(29) Subramaniyan, S.; Xin, H.; Kim, F. S.; Shoaee, S.; Durrant, J. R.; Jenekhe, S. A. *Adv. Energy Mater.* **2011**, *1*, 854.

(30) Faist, M. A.; Kirchartz, T.; Gong, W.; Ashraf, R. S.; McCulloch, I.; de Mello, J. C.; Ekins-Daukes, N. J.; Bradley, D. D. C.; Nelson, J. *J. Am. Chem. Soc.* **2012**, *134*, 685.
(31) Miller, N. C.; Sweetnam, S.; Hoke, E. T.; Gysel, R.; Miller, C. E.; Bartelt, J. A.; Xie, X.; Toney, M. F.; McGehee, M. D. *Nano Lett.* **2012**, *12*, 1566.
(32) Zhang, Z. G.; Zhang, S. Y; Min, J.; Cui, C. H.; Geng, H.; Shuai, Z. G.; Li, Y. F. *Macromolecules* **2012**, *45*, 2312.
(33) He, Y. J.; Zhao, G. J.; Peng, B.; Li, Y. F. *Adv. Funct. Mater.* **2010**, *20*, 3383.
(34) Shoaee, S.; An, Z. S.; Zhang, X.; Barlow, S.; Marder, S. R.; Duffy, W.; Heeney, M.; McCulloch, I.; Durrant, J. R. *Chem. Commun.* **2009**, 5445.
(35) Ohkita, H.; Cook, S.; Astuti, Y.; Duffy, W.; Tierney, S.; Zhang, W.; Heeney, M.; McCulloch, I.; Nelson, J.; Bradley, D. D. C.; Durrant, J. R. *J. Am. Chem. Soc.* **2008**, *130*, 3030.
(36) Arbogast, J. W.; Darmanyan, A. P.; Foote, C. S.; Rubin, Y.; Diederich, F. N.; Alvarez, M. M.; Anz, S. J.; Whetten, R. L. *J. Phys. Chem.* **1991**, *95*, 11.
(37) Guldi, D. M.; Hungerbuhler, H.; Janata, E.; Asmus, K. D. *J. Phys. Chem.* **1993**, *97*, 11258.
(38) Lawson, D. R.; Feldheim, D. L.; Foss, C. A.; Dorhout, P. K.; Elliott, C. M.; Martin, C. R.; Parkinson, B. *J. Phys. Chem.* **1992**, *96*, 7175.
(39) Montanari, I.; Nogueira, A. F.; Nelson, J.; Durrant, J. R.; Winder, C.; Loi, M. A.; Sariciftci, N. S.; Brabec, C. *Appl. Phys. Lett.* **2002**, *81*, 3001.
(40) Clarke, T. M.; Ballantyne, A.; Shoaee, S.; Soon, Y. W.; Duffy, W.; Heeney, M.; McCulloch, I.; Nelson, J.; Durrant, J. R. *Adv. Mater.* **2010**, *22*, 5287.
(41) Clarke, T. M.; Durrant, J. R. *Chem. Rev.* **2010**, *110*, 6736.
(42) Jenekhe, S. A.; Osaheni, J. A. *Science* **1994**, *265*, 765.
(43) Jamieson, F. B. D. E.; MaCarthy Ward, T.; Heeney, M.; Delgado, J.; Martin, N.; Stingelin, N; Durrant, J. *Chem. Sci.* **2012**, *3*, 485.